# EVALUATION OF THE NEURODEGENERATIVE EFFECT OF NANOALUMINUM IN RATS AND THE POTENTIAL THERAPEUTIC EFFECT OF DEFEROXAMINE

***Rehab Mahmoud Mohammad Mhanna[1], Mohamed Mahmoud Nabeh[1], Samar A. Asker[2], Doaa Abdel Wahab El-Morsi[1, 3], and Amal Abd El-Salam El-Bakary[1]***

*[1]Department of Forensic Medicine and Clinical Toxicology, Faculty of Medicine, Mansoura University, Egypt*
*[2]Department of Histology, Faculty of Medicine, Mansoura University, Egypt*
*[3]Department of Medical Education, Delta University for Science and Technology, Egypt*

## ABSTRACT

**Background:** Aluminum nanoparticles (AlNPs) deposition plays a significant role in neurodegenerative disease (NDD) pathogenesis. Deferoxamine (DFO), an iron-chelating agent, shows promise in NDDs. **Aim of the work:** To assess the neurodegenerative toxic effects of AlNPs in rats and evaluate the potential therapeutic effect of DFO. **Material and Methods:** Forty male rats were divided into four groups (n=10). The control group received deionized water for two weeks; the DFO group received 100 mg/kg DFO intraperitoneally daily for seven days; the AlNPs group received 50 mg/kg AlNPs orally for two weeks; the combined group received 50 mg/kg AlNPs for two weeks followed by 100 mg/kg DFO daily for seven days. Amyloid-β and GPx levels were measured, and brain tissues were examined histopathologically. **Results:** There were significant reductions in GPx in the AlNPs group compared to the control and DFO groups (P4<0.001). A significant increase in GPx was observed in the combined group compared to AlNPs alone. Amyloid-β was significantly reduced in the combined group compared to AlNPs. The AlNPs group exhibited significant cerebral, cerebellar, and hippocampal alterations, which returned to near normal with DFO administration. **Conclusion:** Deferoxamine shows potential therapeutic effects in AlNPs-induced NDD, evidenced by reduced cerebral amyloid-β and increased GPx levels, confirmed by near-normal histopathological brain structures post-DFO administration.

**Keywords:** *Aluminum nanoparticles, Amyloid-β, deferoxamine, glutathione peroxidase,*

***Corresponding author:*** *Dr. Rehab Mahmoud Mohammad Mhanna*
*Email: dr_rehabmhann@mans.edu.eg*
ORCID: 0000-0001-9112-4727

## INTRODUCTION

Nanoparticles (NPs) are new synthetic particles with dimensions less than one hundred nanometers (nm). Based on their shape and size, the distinctive physicochemical characteristics give NPs various functions, particularly in the biomedical field ***(Yu et al., 2020)***.

Aluminum oxide ($Al_2O_3$) NPs are a class of metal oxide NPs that have different biomedical applications due to their distinctive physicochemical features, which include resistance to wear and chemicals, and their promising optical features. Further causes for extensive applications include their economical preparation and easy handling ***(Hassanpour et al., 2018)***.

Based on the European Food Safety Authority, a provisional tolerable weekly intake of one milligram of aluminum (Al) per kilogram of body weight (Bw) per week has been confirmed. On the other hand, the European Food Safety Authority has reported that this amount could be exceeded to a major degree by certain people, in particular the pediatric population ***(Aguilar et al., 2008)***.

It has been demonstrated that the adverse effects of ALNPs have been formerly displayed in several studies, while limited data are available as regards their neurotoxic mechanism. Essentially, it has been demonstrated that AlNPs exposure makes the brain more vulnerable to neurodegenerative diseases (NDD), including Alzheimer's disease (AD) ***(Shah et al., 2015)***. Neurodegenerative changes have been recorded to play a primary role in terms of the pathophysiology of several brain disorders. Irrespective of the continuous efforts by current science to make solutions, the outcomes haven't been promising ***(Lamptey et al., 2022)***.

Deferoxamine (DFO) is an iron chelator that suppresses the toxicity of iron or aluminum (Al) and the reactive oxygen species (ROS) that they induce in the body ***(Ballas et al., 2018)***. Such therapeutic medications mainly emerged to evaluate systemic iron overload situations but have since seen considerable development for utilization in cancers ***(Kalinowski and Richardson, 2005)***, imaging ***(Ulaner et al., 2018)***, and neurological disease ***(Masaldan et al., 2019)***.

Regarding the research gap, most prior studies mainly emphasized the neurological adverse effects of AlNPs only.

## THE AIM OF THE WORK

In this study, the neurodegenerative toxic effects of AlNPs and the possible therapeutic role of DFO were evaluated through the measurement of Amyloid-β and glutathione peroxidase (GPX) levels in blood in addition to histopathological study of the brain.

## MATERIAL AND METHODS

The present experimental study was conducted on 40 adult female Albino rats aged three months at the Faculty of Medicine, Mansoura University.

**Study Design:**

Rats were randomly divided into four groups (10 rats in each group). The control group (n=10) received deionized water by oral gavage for two weeks. Deferoxamine (DFO) group (n=10) received daily for seven days with 100 mg/kg DFO intraperitoneally ***(Klebe et al., 2014)*** (could not be taken orally as it is poorly absorbed from the gut) ***(Gavhane and Yadav, 2012)***. The AlNPs group (n=10) received a 50 mg/kg dosage of AlNPs by oral gavage for two weeks ***(OECD, 2001***;***CANLI and Canli, 2017)***.The combined (AlNPs and DFO) group (n=10) received 50 mg/kg dosage of AlNPs by oral gavage for two weeks after 24 hours from the last treatment; rats received 100 mg/kg DFO intraperitoneally daily for seven days; based on the methodologies in ***(OECD, 2001***; ***Klebe et al., 2014***; ***CANLI and Canli, 2017)***.

**Ethical considerations:** The experiment agreed with the Guide on Caring and Using Laboratory Animals (a publication of DHEW (NIH) 8523, 1985) ***(Care and Animals, 1986)***. The present research received ethical approval from the Institutional Research Board of the Faculty of Medicine at Mansoura University *(Code Number: MD.21.03.448).*

**Material:**

The current study used aluminum oxide ($Al_2O_3$) nanoparticles of size <50 nm that were purchased from Sigma Aldrich (No. 702129). One mg/mL concentration of the particles in distilled water was freshly prepared in an ultrasonic water bath and kept in a sonicator for two hours before use.

**Rat Amyloid-β peptide by ELISA kit:** Amyloid-β assay (Cat. No. E0092Ra) kit was purchased from Bioassay Technology Laboratory (China). This kit is an enzyme-linked immunoassay (ELISA).

**Oxidative stress (glutathione peroxidase (GPx) kits:** Glutathione peroxidase (GPx) (Biodiagnostic, Egypt) was measured in the brain tissue of all studied groups as a biomarker for ROS after 24 hours from the last treatment.

**Deferoxamine (DFO):** Deferoxamine was purchased as a vial from Novartis Pharmaceutical Company.

**Sampling:**

Animals were sacrificed 24 hours after the last dose by halothane administration and cervical dislocation, and the next specimens were collected:

a. **Blood samples** by orbital puncture for oxidative stress biochemical studies (GPX) and assessment of amyloid-β peptide level (Due to the utilization of all brain tissue for histopathological examination, GPx and Amyloid-β peptide testing were conducted in blood samples instead).
b. **Brain tissues** for histopathological examination.

**Methods:**

**1. Amyloid-β level assay:**

Amyloid-β level was measured using ELISA technique 24 hours after the last dose in the control group, DFO, and AlNPs groups. In the combined (AlNPs and DFO) group, it was measured after the termination of DFO therapy.

**2. Glutathione peroxidase:**

It provides specific and mechanistic insights into how cells respond to Amyloid-β-induced oxidative stress ***(Sultana and Butterfield, 2010; Butterfield and Halliwell, 2019)***.

**Histopathological examination:**

The brain tissues were extracted and examined histopathologically by Hx and E after 24 hours from the end of the experiment.

**Statistical Analysis:**

Data analysis was conducted by using SPSS software (PASW statistics for Windows version 25. Chicago). Qualitative data were defined by utilizing numbers and percentages. Quantitative data were described by utilizing mean±SD for normally distributed data, following testing normality by utilizing the Shapiro-Wilk test. The significance of the results was judged at the (≤0.05) level. A one-way ANOVA test was utilized for comparison of at least 3 independent groups with a post hoc Tukey test to determine pairwise comparison. The Spearman's correlation was used to detect the strength as well as the direction of a linear correlation between two non-normally distributed variables.

## RESULTS

By comparing the mean values of glutathione peroxidase (GPx) level among all the studied groups, there were high statistically significant reductions in GPx in the AlNPs group compared to the control group and DFO group. Additionally, a significant increase in GPx level was recorded in the combined (AlNPs and DFO) group compared to AlNPs only **(Table 1)**.

Regarding the mean values of Aβ peptide among all the studied groups, there was a statistically significant increase in Aβ peptide in the AlNPs group compared to the control group (P2=0.048) and DFO group (P4=0.01). Additionally, significant reduction in Aβ peptide was recorded in the combined (AlNPs and DFO) group compared to the AlNPs group (P6=0.004) **(Table 2)**.

By studying the correlation between amyloid-β peptide and GPX within each of the studied groups, there was a high statistically significant negative correlation between amyloid-β peptide and GPx in the combined (AlNPs and DFO) group (P<0.001), while no significant correlations were recorded regarding all the remaining groups (P>0.05) **(Table 3)**.

**Table (1): Comparison between the mean values of glutathione peroxidase (GPx) (U/g hemoglobin) among all the studied groups (n=40).**

| | Control group (n=10) | DFO group (n=10) | AlNPs group (n = 10) | Combined (AlNPs and DFO) group (n = 10) | Test of significance | Significance between groups |
|---|---|---|---|---|---|---|
| **GPx mean±SD (U/g hemoglobin)** | 62.17±6.33 | 57.34±6.15 | 40.27±13.55 | 49.31±9.98 | F=10.21<br>P<0.001* | P1=0.263<br>P2<0.001*<br>P3=0.005*<br>P4<0.001*<br>P5=0.067<br>P6=0.04* |

*SD: Standard deviation, DFO: Deferoxamine, AlNPs: Aluminum nanoparticles, GPx: glutathione peroxidase, n:number, F:One Way ANOVA test , *statistically significant when P value<0.05.*

*P1: Difference between control group and DFO group.*

*P2: Difference between control group and AlNPs group.*

*P3: Difference between control group and combined (AlNPs and DFO) group.*

*P4: Difference between DFO group and AlNPs group).*

*P5: Difference between DFO group and combined (AlNPs and DFO) group.*

*P6: Difference between AlNPs group and combined (AlNPs and DFO) group.*

**Table (2): Comparison between the mean values of amyloid-β peptide (pg/mL) among all the studied groups (n=40).**

| | Control group (n=10) | DFO group (n=10) | AlNPs group (n=10) | Combined (AlNPs and DFO) group (n=10) | Test of significance | Significance between groups |
|---|---|---|---|---|---|---|
| **Amyloid-β peptide mean±SD (pg/mL)** | 0.1132±0.01 | 0.1055±0.037 | 0.136±0.012 | 0.102±0.028 | F=2.67<br>P=0.062 | P1=0.493<br>P2=0.048*<br>P3=0.308<br>P4=0.01*<br>P5=0.734<br>P6=0.004* |

*SD: Standard deviation, DFO: Deferoxamine, AlNPs: Aluminum nanoparticles, n: number, F: One Way ANOVA test, *statistically significant when P value<0.05.*
*P1: Difference between control group and DFO group.*
*P2: Difference between control group and AlNPs group.*
*P3: Difference between control group and combined (AlNPs and DFO) group.*
*P4: Difference between DFO group and AlNPs group).*
*P5: Difference between DFO group and combined (AlNPs and DFO) group.*
*P6: Difference between AlNPs group and combined (AlNPs and DFO) group.*

**Table (3): Correlation between amyloid-β peptide and glutathione peroxidase within each of the studied groups.**

| Groups | Correlation | Amyloid-β and GPx |
|---|---|---|
| **Control group (n = 10)** | r | -.239 |
| | p | 0.506 |
| **DFO group (n = 10)** | r | 0.095 |
| | p | 0.795 |
| **AlNPs group (n = 10)** | r | -.625 |
| | p | 0.054 |
| **Combined (AlNPs and DFO) group (n = 10)** | r | -.997** |
| | p | <0.001** |

*AlNPs: Aluminum nanoparticles, DFO Deferoxamine, GPx: glutathione peroxidase, n=number, r: Spearman correlation coefficient, **statistically significant when P value<0.05.*

**Histopathological results (H&E):**

Microscopic examination of H&E-stained sections of the cerebral cortex from the frontal area of both the control and the DFO groups of rats shows the normal cerebral cortex structure. They reveal 6 layers. The common cells of these layers are the pyramidal, granular, and neuroglial cells **(Figure 1)**.

Examination of sections obtained from AlNPs group rats shows severe disorganized general histological structure of the cortex compared to the control group and DFO group. The pia matter shows many dilated congested blood vessels surrounded by many inflammatory cells. There are cracks, many vacuoles, aggregation of cells and fibers, and degenerated nerve fibers (gliosis) **(Figure 2 A-C)**. Some pyramidal cells show faint nuclei or darkly stained nuclei and are bounded by vacuolated neuropil **(Figure 2D)**.

Examination of sections acquired from the combined (AlNPs and DFO) group rats, is more or less as that of control group. On the other hand, occasional pyramidal cells are still affected. They are shrunken, had darkly stained nuclei and pericellular halos and the neuropil remains vacuolated **(Figure 3)**.

Moreover, microscopic examination of H andE stained sections of the hippocampus of control group and DFO group rats demonstrates the distinctive areas of hippocampal formation. These are the hippocampus proper, dentate gyrus (DG) and subiculum. The hippocampus proper is composed of Cornu Ammonis (CA) CA1 and CA2, which consist of a zone of small pyramidal cells; CA3 and CA4 form a zone of large pyramidal cells. CA4 projects into DG concavity consist of small granule cells. Subiculum is a continuation of the CA1 region.

Areas in between compact zones of cells include the ML **(Figure 4A)**.

Sections from AlNPs group rats are markedly affected show dilated congested blood vessels in the neuropil and in the substance of the hippocampus. The thicknesses of the small pyramidal cell layers (PCL) are decreased

with many degenerated cells with dark nuclei are seen. Many glial cells surrounding the pyramidal cells are detected **(Figure 4B)**.

Examination of sections obtained from the combined (AlNPs and DFO) group: most of which are similar to the control group. However, pia matter shows some dilated congested blood vessels, also few vacuolation and glial cells are present in the pyramidal layer **(Figure 4C)**.

Microscopic examination of H and E-stained sections of the cerebellum of control group and DFO group rats shows the normal structure of the cerebellum. They reveal three layers from outside inwards of the cortex. The common cells of these layers are the Purkinje cells, granule cells, and neuroglial cells **(Figure 5A)**.

Examination of the cerebellar sections obtained from AlNPs group rats reveals congested blood vessels and inflammatory cells are detected in the epidura adjacent to the cerebellar folia. The Purkinje cell layer shows many vacuoles with distorted Purkinje cells, cellular shrinkage, and karyorrhexis of some nuclei. The glomeruli appeared shrunken. Empty spaces are detected due to the increased valcuolation in the neuropil tissue **(Figure 5B)**. Examination of sections obtained from the combined (AlNPs and DFO) group is similar to the control group **(Figure 5C)**.

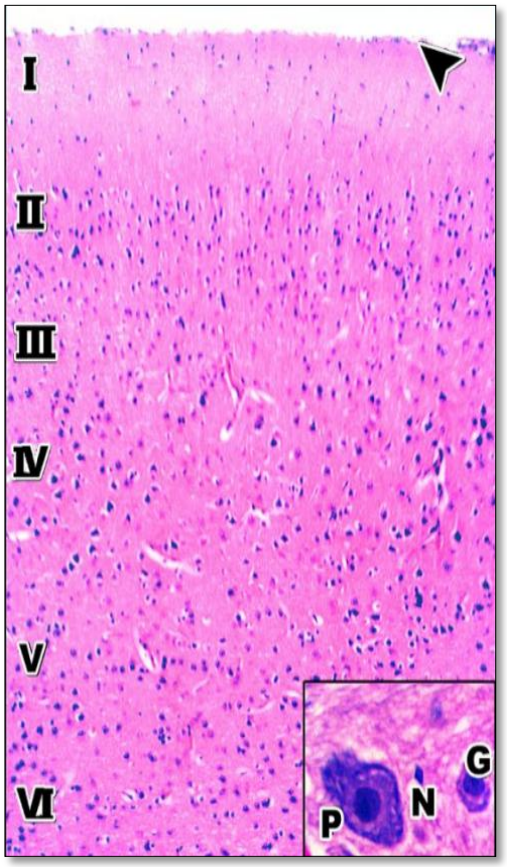


***Figure (1):*** *A photomicrograph of a cerebral cortex section of a control rat shows the general cerebral cortex histologic structure. The pia matter (arrow), molecular layer (ML) (I), external granular layer (EGL) (II), external pyramidal layer (EPL) (III), inner granular layer (IGL) (IV), inner pyramidal layer (IPL) (V), and multiform layer (VI). Inset shows pyramidal cell (P), granule cell (G), and neuroglia (N) (H&E X100) (inset X 1000).*

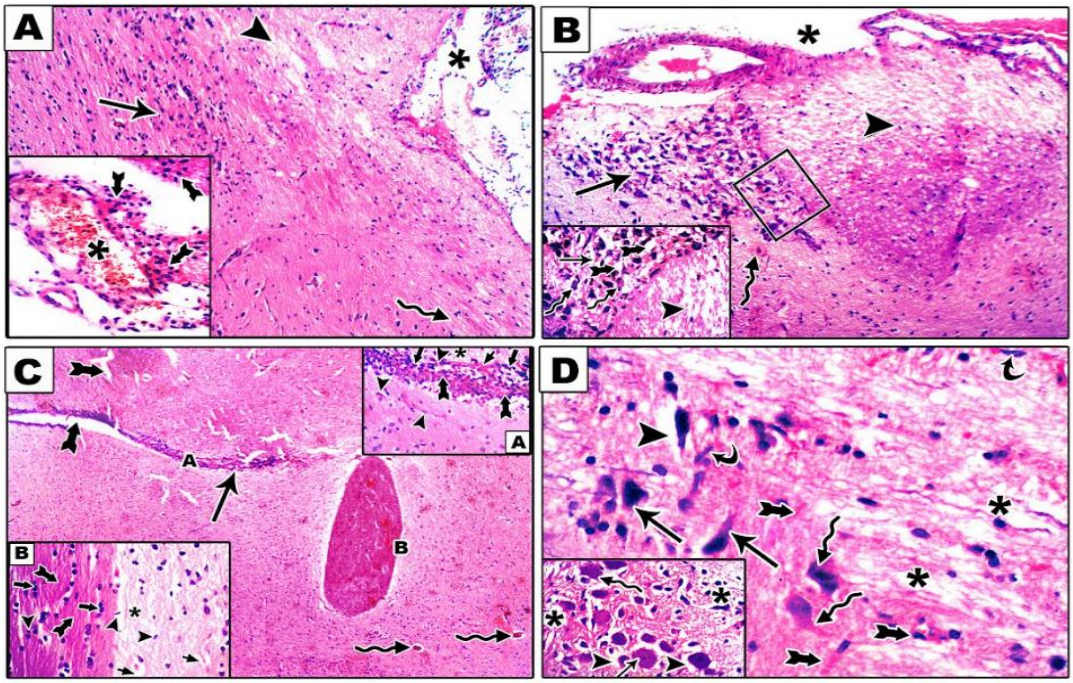


***Figure (2):*** *A photomicrograph of a section in the cerebral cortex of the AlNPs group shows (AandB) disorganized general histologic structure of the cerebral cortex in the form of many vacuoles (head arrow), aggregation of cells (arrow) and fibers (zigzag arrow). The pia matter shows many dilated congested blood vessels (star) surrounded by many inflammatory cells (tailed arrow). (H&E X100) (inset X 400) (B) The inset shows degenerated nerve fibers (zigzag arrow), congested blood vessels (arrows) and vacuoles (tailed arrow). In addition, there are dilated congested blood vessels in the pia matter (star). (H&E X200) (inset X 400). (C) Shows disorganized general histologic structure of the cortex in the form of cracks in different areas (tailed arrows) and many congested blood vessels (zigzag arrows). Notice, two parts (AandB) of aggregated nerve cells and fibers (gliosis) in the substance of the cortex. The inset (AandB) shows vacuolated neuropil (*) with many congested blood vessels (short arrows), darkly stained neuroglial cells (thick arrows) and microglia (arrow heads). Many acidophilic fibers (tailed arrows) are noticed between the neuroglia cells. (H&E X100) (inset X 400). (D) shows irregular pyramidal cells their nuclei appear faint like ghosts (zigzag arrow) others have darkly stained nuclei (arrows) while others are surrounded by vacuolated neuropil (arrow heads). Many neuroglia cells (curved arrows) and congested blood vessels (tailed arrows) are seen in the vacuolated neuropil (*) (H&E X400).*

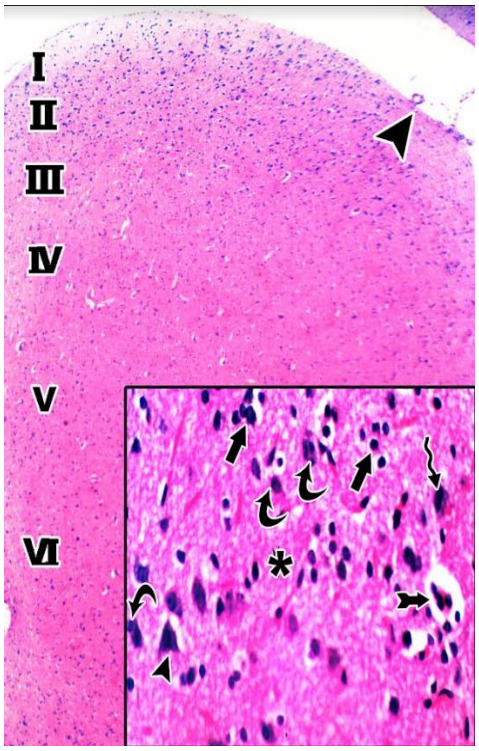


***Figure (3):*** *A photomicrograph of a section in the cerebral cortex of AL+D rat shows the general cerebral cortex histologic structure. The pia matter has no congested blood vessels (arrow head), ML (I), EGL (II), EPL (III), IGL (IV), IPL (V) and the multiform layer (VI). Inset shows certain pyramidal cells with dark nuclei and surrounded with regular neuropil (zigzag arrow) others with vacuolated neuropil (arrow head). Some pyramidal cells are degenerated (curved arrows). The neuropil is regular (*) but contains congested blood vessels (tailed arrows) and aggregated neuroglia (thick arrows) (H&E X100) (inset X 400).*

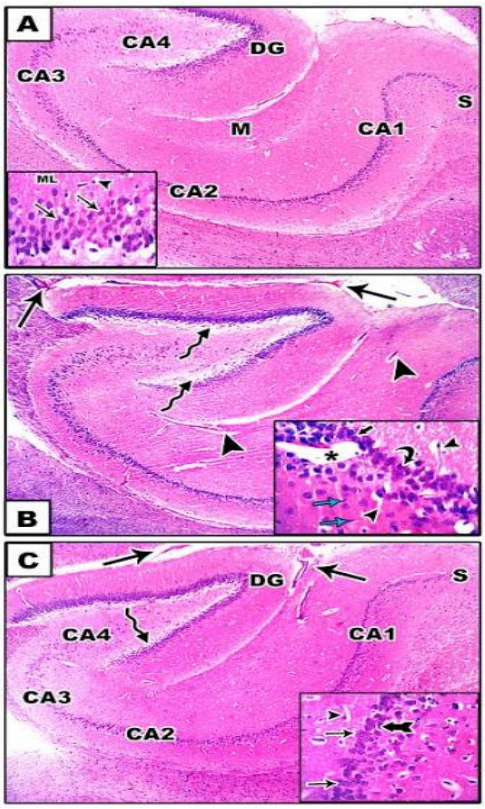


***Figure(4):*** *(A) A photomicrograph of a section in the section of control rats shows the different areas of the hippocampus proper, which consists of the CA as CA1, CA2, CA3, and CA4 regions, and is continued as subiculum (S). In addition, DG is detected adjacent to CA4 by its limbs. Inset shows ML with few blood vessels (arrow head). Small pyramidal cells of the CA1 region form 5–6 compact layers with vesicular nuclei (arrows). (B) A photomicrograph of a section in the section of the AlNPs group rats shows dilated congested blood vessels in the neuropil (arrows) and in the substance of the hippocampus (arrow heads). The pyramidal layer shows many vacuolations (zigzag arrow). Inset shows dilated blood vessel within the pyramidal layer (*) and reduced thickness of layer of pyramidal cells of CA1 to reach two layers in certain areas (curved arrow). Many degenerated cells with dark nuclei are seen (thick arrow). Microglia surround the pyramidal cells (blue arrow). (C) A photomicrograph of a section of the combined group (AlNPs and DFO) rats shows the different areas of the hippocampus proper, which consists of the CA as CA1, CA2, CA3, and CA4 areas and is continued as subiculum (S). In addition, DG could be detected surrounding CA4 by its limbs. The pia matter shows many dilated congested blood vessels (arrows) and few vacuolation are present in the pyramidal layer (zigzag arrow). Inset shows ML with few blood vessels (arrow head). Small pyramidal cells of the CA1 region form 5–6 compact layers with vesicular nuclei (arrows). Some microglia surround the* pyramidal cells (tailed arrow) (H&E X100) (inset X 400).

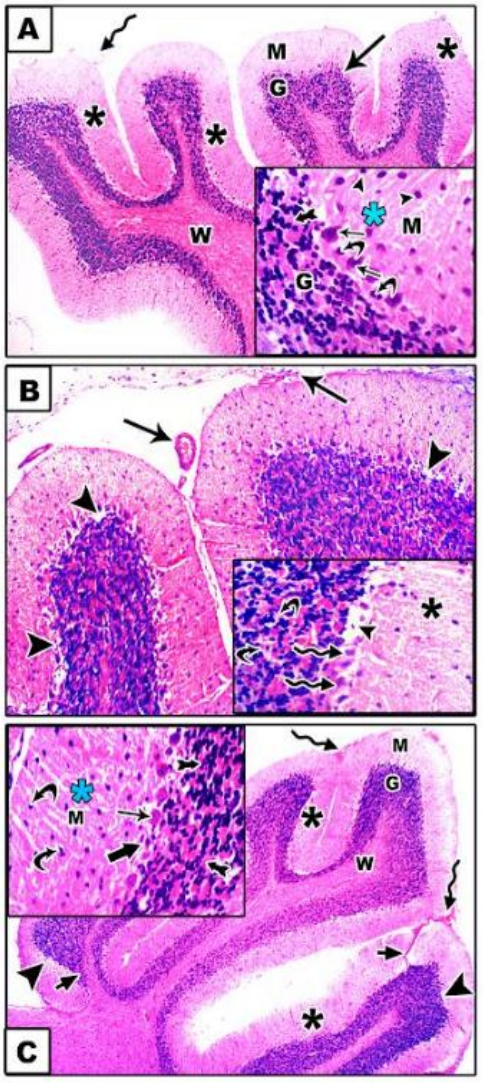


***Figure (5):*** *A photomicrograph of a section in the cerebellum shows (A) cerebellar folia (*) of control rats consist of cortex and white matter (W), which are surrounded by epidura with non-congested blood vessels (zigzag arrow). The cortex consists of ML (M), Purkinje cells layer (arrow), and granular layer (G). The Purkinje cell layer comprises a single row of large flask-shaped cells (these cells have regular arrangements) with vesicular nuclei (arrows), which are surrounded with Bergmann glia astrocytes that show vesicular nuclei (curved arrows). The granular layer contains small granule cells with dark nuclei (G) which surround homogenous eosinophilic glomeruli (tailed arrow). The neuropil is homogenous with a mild extracellular vacuolations (*) [H&E x 40, inset x400]. (B) Cerebellum of the AlNPs group rats shows congested blood vessels and inflammatory cells (arrows) are detected in the epidura nearby the cerebellar folia. The Purkinje cell layer shows many vacuoles (arrow heads). The inset shows distorted Purkinje cells with cellular shrinkage and karyorrhexis of some nuclei (zigzag arrows). The glomeruli between granule cells appear shrunken (curved arrows). Empty spaces are detected due to the increased valcuolation in the neuropil tissue (*). [H&E x 100, inset x400]. (C) The cerebellum of the combined group (AlNPs and DFO) shows cerebellar folia (*) composed of cortex and white matter (W), which are surrounded by epidura with some congested blood vessels (zigzag arrow). The cortex is formed of; ML (M) with some congested blood vessels (short arrows), Purkinje cells layer shows vacuolation in some areas (arrowheads), and granular layer (G). Inset shows the ML (M) with glial cells nuclei (curved arrows). The Purkinje cell layer comprises one row of regularly arranged large flask-shaped cells with vesicular nuclei (arrow) which are surrounded with Bergmann glia astrocytes (thick arrow). The granular layer contains small granule cells with dark nuclei which surround homogenous eosinophilic glomeruli (tailed arrow). The neuropil is homogenous with a minimal extracellular vacuolations (*) [H&E x 40, inset x400].*

## DISCUSSION

The current study objective was to assess the neurodegenerative toxic effects of AlNPs in albino rats through the measurement of amyloid-β peptide and GPx levels in blood in addition to histopathological study of the brain. Furthermore, the potential therapeutic effects of DFO were evaluated.

The current results showed that AlNPs-induced a significant reduction in glutathione compared to control values. This reduction of glutathione levels was significantly improved after administration of DFO for seven days, but did not return to control values.

Likewise, ***Abdelhameed et al. (2023)*** carried out a study on 40 adult male Wistar rats to evaluate the toxic actions of AlNPs and the possible therapeutic role of melatonin. They have demonstrated that AlNPs-treated rats at a dose of 30 mg/kg Bw for four weeks (oral gavage) were accompanied by a significant increase in malondialdehyde (MDA) levels and a significant reduction in glutathione levels.

Also, ***M'rad et al. (2018)*** stated that after the exposure to AlNPs, an increase in MDA levels with an associated reduction in superoxide dismutase level was detected which established the initiation of oxidative stress in the hippocampus. However, there were no changes in the thiol group levels or the activities of catalase and GPx.

Similarly, ***Prabhakar et al. (2012)*** assessed the oxidative stress caused following acute oral treatment with 500, 1000, and 2000 mg kg−1 doses of $Al_2O_3$−30 and −40 nm and bulk (macro-scale particles) $Al_2O_3$ in Wistar rats. Both the NPs (30 nm and 40 nm) caused significant increases in oxidative stress compared to the bulk. Both NPs (30 nm and 40 nm) demonstrated an insignificant difference.

In the same line, ***Shah et al. (2015)*** noticed that, contrasting to untreated control cells, AlNPs-treated cells were associated with a significant increase in ROS in both human neuroblastoma and mouse hippocampal cells after exposure for six hours.

Some authors explained the AlNPs-induced oxidative stress by the induction of mitochondrial disruption and depletion of the mitochondrial thiols, stimulating apoptotic caspases (IX and III) with a subsequent alteration of antioxidant enzyme expression, generating more ROS ***(M'rad et al., 2018)***.

In this context, DFO was able to reduce oxidative stress. It was suggested that DFO might suppress the formation of free radicals ***(Kletkiewicz et al., 2016)***.

The current study demonstrated that AlNPs induced a significant increase in amyloid-β peptide (1-40) (the major C-terminal variants of the Aß protein demonstrating neurodegeneration; 1-40 indicates the length of the amino acid chain). However, following DFO administration in AlNPs treated rats; amyloid-β (1-40) was significantly reduced to reach average control levels.

Likewise, ***Abdelhameed et al. (2023)*** demonstrated that AlNPs significantly increased amyloid-β peptide in their studied rates.

The theory that Al is a risk factor for AD pathogenesis, called the "aluminum hypothesis," was suggested in the 1960s according to different neurological, toxicological, and epidemiological outcomes ***(Klatzo et al., 1965)***. Despite these outcomes, the Al hypothesis has been the topic of great controversy for many years. As a result, more efforts have been conducted in terms of AD studies. In particular, much research has reinforced the notion called "amyloid cascade hypothesis," namely that the conformational alterations of amyloid-β and its neurotoxic effect have a main role in the context of AD pathogenesis ***(Hardy and Selkoe, 2002; Wirths et al., 2004)***.

Aluminum and other metals such as zinc, copper, and iron affect the oligomerization and conformational alterations of Aβ, and, as a result, their effects are essential in such sitting. In addition, there is growing evidence that these metals may have an impact on the pathophysiology of AD. Aluminum binds to different metal-binding proteins and affects the homeostasis of different metals ***(Wirths et al., 2004)***.

As for DFO, it was found that DFO plays an essential role in the treatment of AlNPs–induced neurofibrillary degeneration via inhibition of Aβ depositing in the amyloid precursor protein /presenilin-1 (APP/ PS1) in the mouse brain ***(Zhaba et al., 2021)***.

In addition, DFO could significantly decrease cerebral amyloid-β following head trauma in mice ***(Zhaba et al., 2021)***.

As regards the correlation between amyloid-β peptide and GPx, the present study revealed that there was a highly significant negative correlation between amyloid-β peptide and GPx in the combined (AlNPs and DFO) group.

Essentially, oxidative stress and amyloid-β are linked to each other because amyloid-β induces oxidative stress; oxidative stress increases the amyloid-β deposition. As a result, the answer to the question "Which comes first: the chicken or the egg?" is still really challenging ***(Tamagno et al., 2021)***.

Of note, there is evidence indicating that a long-term period of gradual oxidative damage accumulation comes first and causes Aβ accumulation, the development of neurofibrillary tangles (NFTs), and impairment of metabolic and cognitive functions ***(Tamagno et al., 2021)***.

Oxidative stress, which happens within the bilayer and is theorized in the Aβ-induced oxidative stress theory, has been demonstrated to start the process of lipid peroxidation ***(Butterfield et al., 2013)***.

Besides, AD is associated with an imbalance in iron homeostasis. Excessive iron participates in amyloid-β deposition with a subsequent formation of NFTs, which ultimately promotes AD development. Hence, iron-targeted therapeutic modalities have become a novel direction, which includes DFO ***(Liu et al., 2018)***.

Concerning histopathologic examination, the AlNP group showed a disorganized histologic structure of the cerebral cortex, hippocampus, and cerebellum. There were many congested blood vessels. There were aggregated nerve cells and fibers (gliosis) in the substance of the cortex and the inset shows vacuolated neuropil with many congested blood vessels, darkly stained neuroglial cells and microglia. The inset of hippocampus shows dilated blood vessel within the pyramidal layer and diminished PCL thickness of CA1 to reach two layers in certain regions. The inset of the cerebellum shows distorted Purkinje cells with cellular shrinkage and karyorrhexis of some nuclei.

Likewise, ***Abdelhameed et al. (2023)*** observed in their study that AlNPs-induced severe histopathological changes, such as neuropil vacuolation, enlargement of perivascular spaces, vascular congestion, neurodegenerative changes, and pyknosis. In addition, treatment of AlNPs has been demonstrated to be associated with extensive positive caspase-3 immunostaining.

The present results augment the results of ***Shah et al. (2015)***, who demonstrated that AlNPs (by intraperitoneal injection) given to female mice for 21 days increased brain aluminum, disturbed cerebral energy homeostasis, and caused impaired hippocampus-dependent memory. Essentially, such NPs caused AD neuropathology by improving the amyloidogenic pathway of Aβ formation and aggregation and indicated the advancement of cortical and hippocampal neurodegenerative changes in these mice.

Also, ***Sun et al. (2022)*** found that AlNPs accumulation in the hippocampus excessively stimulates pro Brain-derived neurotrophic factor (proBDNF) signaling, with a subsequent impairment of neurons and memory.

In the same line, ***Singh et al. (2018)*** displayed that; cortical and hippocampal histological examination of aluminum chloride-exposed rat brains revealed the existence of neuritic plaques and NFTs.

Also, ***M'rad et al. (2018)*** demonstrated that exposure to AlNPs caused diminished acetylcholinesterase activity in the hippocampus. In addition, AlNPs facilitated Al deposition and disturbed mineral element homeostasis in the hippocampus. On the other hand, they could not prove any changes in the hippocampal shape. In addition, their outcomes showed a relationship among oxidative stress, disturbance of mineral homeostasis, and aluminum deposition in the hippocampus, with subsequent impairment of memory in AlNPs-treated rats.

***Chen et al. (2008)*** suggested that, administration of AlNPs was associated with a marked disturbance of the integrity of claudin-V and occludin (tight junction proteins; their dysfunction has been implicated in NDD). These data explain the effects of AlNPs on cerebral vasculature.

On the other hand, ***Prabhakar et al. (2012)*** could not demonstrate any histopathological changes in the brain following acute oral treatment with 500, 1000, and 2000 mg kg−1 doses of nano Al2O3 -30 and −40 nm, and bulk $Al_2O_3$ (macro-scale) in Wistar rats. This could be explained by the different study design. In their study they assessed the toxic effects of acute oral ingestion only; however, the current study used AlNPs for 14 days (in other words, subacute exposure).

Interestingly, the current study demonstrated that following DFO administration to AlNPs-received rats, there was a marked improvement as regards histopathological results. Most rats were more or less like those of the control group. There was a marked reduction in blood vessel congestion. However, a few pyramidal cells remained affected.

To our knowledge, this is the first study that used DFO in the treatment of AlNPs-induced neurodegeneration.

However, after traumatic brain injury (TBI) in mice, ***Zhang and He (2017)*** demonstrated that DFO significantly improved cognitive function and deposition of Aβ and suppressed cerebral apoptosis. In addition, DFO induced M2 activation of microglia (M2 microglia produce anti-inflammatory cytokines and growth factors that encourage reduction of the inflammatory response and repair of damaged tissue) and suppressed M1 activation of microglia in the hippocampus of APP/PS1 mice (M1 microglia release inflammatory cytokines and chemokines, causing inflammation and neuronal death).

To conclude, GPx and the histopathological changes did not return to normal control levels, while amyloid-β returned to normal control levels after DFO administration for seven days to AlNPs (at a dose of 50 mg/kg and a size of <50 nm) exposed rats for 14 days.

**Limitations of the study:**

Despite the previously promising results, in terms of the effects of DFO on experimental animal models, there are still numerous problems related to its clinical application. First, the oral bioavailability of DFO is poor. Second, the time of a single IV infusion is long (about ten hours), and the frequency of the IV infusion is high, resulting in low patient compliance. In addition, it has several potential adverse effects, including neurotoxicity, anemia, and gastrointestinal malabsorption.

While there are potential alternatives to DFO, these agents may also have their own limitations; regarding their availability, and lack the extensive preclinical data supporting their efficacy.

## CONCLUSION

Aluminum NPs administration induced marked neurodegeneration in rats. Deferoxamine has a potential therapeutic role in the context of AlNPs-induced NDD as revealed by the reduction in amyloid-β level. The reduction of oxidative stress seemed to be a potential mechanism. These data were confirmed by histopathological alteration of the cortex, hippocampus, and cerebellum, which returned to near normal following DFO administration.

## RECOMMENDATIONS

The current study could open avenues toward the utilization of DFO as a talented agent in the context of NDD-affected cases such as (AD). Further studies have to be conducted in the future comparing the effectiveness of DFO and other iron chelators such as deferasirox and deferiprone.

**Conflict of interest:** None.

**Sources of funding:** None.

## REFERENCES

1. **Abdelhameed, N. G.; Ahmed, Y. H.; Yasin, N. A. et al. (2023):** Effects of Aluminum Oxide Nanoparticles in the Cerebrum, Hippocampus, and Cerebellum of Male Wistar Rats and Potential Ameliorative Role of Melatonin. *ACS Chem. Neurosci., 14*(3)*: 359-369.*
2. **Aguilar, F.; Autrup, H.; Barlow, S. et al. (2008):** Safety of aluminium from dietary intake scientific opinion of the panel on food additives, flavourings, processing aids and food contact materials (AFC). *EFSA J., 754: 1-34.*
3. **Ballas, S. K.; Zeidan, A. M.; Duong, V. H. et al. (2018):** The effect of iron chelation therapy on overall survival in sickle cell disease and β thalassemia: A systematic review. *Amer. J. Hematol., 93(7): 943-952.*

4. **Butterfield, D. A.; and Halliwell, B. (2019):** Oxidative stress, dysfunctional glucose metabolism and Alzheimer disease. *Nature Rev. Neurosci., 20*(3)*: 148-160.*
5. **Butterfield, D. A.; Swomley, A. M. and Sultana, R. (2013):** Amyloid β-peptide (1–42)-induced oxidative stress in Alzheimer disease: importance in disease pathogenesis and progression. *Antiox. Redox Sign., 19(8): 823-835.*
6. **CANLI, E. G. and Canli, M. (2017):** Effects of aluminum, copper, and titanium nanoparticles onsome blood parameters in Wistar rats. *Turkish J. Zool., 41(2): 259-266.*
7. **Care, I. o. L. A. R. C. o. and Animals, U. o. L. (1986):** Guide for the care and use of laboratory animals: US Department of Health and Human Services, *Public Health Service, National Institute of Health.*
8. **Chen, L.; Yokel, R. A.; Hennig, B. et al. (2008):** Manufactured aluminum oxide nanoparticles decrease expression of tight junction proteins in brain vasculature. *J. Neuroimm. Pharmacol., 3*:*286-295.*
9. **Gavhane, Y. N. and Yadav, A. V. (2012):** Loss of orally administered drugs in GI tract. *Saudi Pharmaceut.J., 20(4): 331-344.*
10. **Hardy, J. and Selkoe, D. J. (2002):** The amyloid hypothesis of Alzheimer's disease: Progress and problems on the road to therapeutics. *Sci., 297*(5580)*:353-356.*
11. **Hassanpour, P.; Panahi, Y.; Ebrahimi- Kalan, A. et al. (2018):** Biomedical applications of aluminium oxide nanoparticles. *Micro Nano Lett., 13*(9)*: 1227-1231.*
12. **Kalinowski, D. S. and Richardson, D. R. (2005):** The evolution of iron chelators for the treatment of iron overload disease and cancer. *Pharmacol. Rev., 57*(4)*: 547-583.*
13. **Klatzo, I.; Wiśniewski, H. and Streicher, E. (1965):** Experimental production of neurofibrillary degeneration: I. Light microscopic observations. *J. Neuropathol. Exp. Neurol., 24(2): 187-199.*
14. **Klebe, D.; Krafft, P. R.; Hoffmann, C. et al. (2014):** Acute and delayed deferoxamine treatment attenuates long-term sequelae after germinal matrix hemorrhage in neonatal rats. *Stroke, 45(8): 2475-2479.*
15. **Kletkiewicz, H.; Nowakowska, A.; Siejka, A. et al. (2016):** Deferoxamine improves antioxidative protection in the brain of neonatal rats: The role of anoxia and body temperature. *Neurosci. Lett., 628: 116-122.*
16. **Lamptey, R. N.; Chaulagain, B.; Trivedi, R. et al. (2022):** A review of the common neurodegenerative disorders: current therapeutic approaches and the potential role of nanotherapeutics. *Int. J. Molec. Sci., 23(3): 1851.*
17. **Liu, J. L.; Fan, Y. G.; Yang, Z. S. et al. (2018):** Iron and Alzheimer's disease: from pathogenesis to therapeutic implications. *Front. Neurosci., 12(1):632.*
18. **M'rad, I.; Jeljeli, M.; Rihane, N. et al. (2018):** Aluminium oxide nanoparticles compromise spatial learning and memory performance in rats. *EXCLI J., 17: 200.*
19. **Masaldan, S.; Bush, A. I.; Devos, D. et al. (2019):** Striking while the iron is hot: Iron metabolism and ferroptosis in neurodegeneration. *Free Rad. Biol. Med., 133:221-233.*
20. **OECD (2001):** Guideline 423: Guideline for testing of chemicals: acute oral toxicity-acute toxic class method, *OECD Paris. pp. 17.*
21. **Prabhakar, P.; Reddy, U. A.; Singh, S. et al. (2012):** Retracted: Oxidative stress induced by aluminum oxide nanomaterials after acute oral treatment in Wistar rats. *J. App.Toxicol., 32(6): 436-445.*
22. **Shah, S. A.; Yoon, G. H.; Ahmad, A. et al. (2015):** Nanoscale-alumina induces oxidative stress and accelerates amyloid beta (Aβ) production in ICR female mice. *Nanoscale, 7(37): 15225-15237.*
23. **Singh, N. A.; Bhardwaj, V.; Ravi, C. et al. (2018):** EGCG nanoparticles attenuate aluminum chloride induced neurobehavioral deficits, beta amyloid and tau pathology in a rat model of Alzheimer's disease. *Front. Aging Neurosci., 10: 244.*
24. **Sultana, R. and Butterfield, D. A. (2010):** Role of oxidative stress in the progression of Alzheimer's disease. *J. Alzheimer's Dis., 19(1): 341-353.*
25. **Sun, W.; Li, J.; Li, X. et al. (2022):** Aluminium oxide nanoparticles compromise spatial memory performance and proBDNF-mediated neuronal function in the hippocampus of rats. *Particle Fibre Toxicol., 19(1): 1-14.*
26. **Tamagno, E.; Guglielmotto, M.; Vasciaveo, V. et al. (2021):** Oxidative stress and beta amyloid in Alzheimer's disease. Which comes first: The chicken or the egg? *Antiox., 10(9): 1479.*

27. **Ulaner, G. A.; Lyashchenko, S. K.; Riedl, C. et al. (2018):** First-in-human human epidermal growth factor receptor 2–targeted imaging using 89Zr-Pertuzumab PET/CT: dosimetry and clinical application in patients with breast cancer. *J. Nucl. Med., 59(6): 900-906.*

28. **Wirths, O.; Multhaup, G. and Bayer, T. A. (2004):** A modified β amyloid hypothesis: intraneuronal accumulation of the β amyloid peptide–the first step of a fatal cascade. *J. Neurochem., 91(3): 513-520.*

29. **Yu, Z.; Li, Q.; Wang, J. et al. (2020):** Reactive oxygen species-related nanoparticle toxicity in the biomedical field. *Nanoscale Res. Lett., 15(1): 1-14.*

30. **Zhaba, W.-D.; Deji, Q.-Z.; Gao, S.-Q. et al. (2021):** Deferoxamine reduces amyloid-beta peptides genesis and alleviates neural apoptosis after traumatic brain injury. *Neuroreport, 32(6): 472-478.*

31. **Zhang, Y. and He, M.-l. (2017):** Deferoxamine enhances alternative activation of microglia and inhibits amyloid beta deposits in APP/PS1 mice. *Brain Res., 1677: 86-92.*